Selection Optimization in the Search for Supersymmetry in Events with Three Leptons and Missing Transverse Momentum with the ATLAS Detector at the LHC and at the HL-LHC

Kyle Boone

Supervisor: Dr. Colin Gay

CERN Summer Student Program 2012

The University of British Columbia

ATLAS

September 11, 2012

Abstract

A supersymmetry model was investigated where the only light superparticles are weak gauginos. In such a model, the production of $\tilde{\chi}_2^0\tilde{\chi}_1^\pm$ can be observed by its decay via a W and a Z boson to a final state with 3 leptons and missing transverse energy. Samples were generated using Monte Carlo generators and multivariate techniques were used to optimize the signal selection. The results were interpreted as discovery and exclusion reaches for the 2012 search for this model. A similar study was performed for both the full LHC run and the proposed HL-LHC run and interpreted as discovery and exclusion reaches.

Table 1: Particles in the MSSM grouped by charge

Standard model particle	Corresponding MSSM particle	Mass eigenstate
quark (u, d, s, c, b, t)	squark $(\tilde{u}, \tilde{d}, \tilde{s}, \tilde{c}, \tilde{b}, \tilde{t})$	
lepton (e, μ, τ)	slepton $(\tilde{e}, \tilde{\mu}, \tilde{\tau})$	
neutrino $(\nu_e, \nu_{mu}, \nu_\tau)$	sneutrino $(\tilde{\nu}_e, \tilde{\nu}_{mu}, \tilde{\nu}_\tau)$	
gluon (g)	gluino $(\tilde{g})$	
neutral Higgs bosons (H_u^0, H_d^0)	neutral higgsinos $(\tilde{H}_u^0, \tilde{H}_d^0)$	neutralinos $(\tilde{\chi}_1^0, \tilde{\chi}_2^0, \tilde{\chi}_3^0, \tilde{\chi}_4^0)$
neutral W boson (W^0)	neutral wino $(\tilde{W}^0)$	
B boson (B^0)	bino $(\tilde{B}^0)$	
charged Higgs bosons (H_u^+, H_d^-)	charged higgsinos $(\tilde{H}_u^+, \tilde{H}_d^-)$	charginos $(\tilde{\chi}_1^+, \tilde{\chi}_1^-, \tilde{\chi}_2^+, \tilde{\chi}_2^-)$
charged W bosons (W^+, W^-)	charged winos $(\tilde{W}^+, \tilde{W}^-)$	

1 Introduction

1.1 Supersymmetry

Supersymmetry (SUSY) is one of the most promising theories for physics beyond the standard model. In supersymmetric models, each standard model particle has a corresponding superpartner with spin differing by 1/2. Supersymmetry can provide both a solution to the hierarchy problem and a dark matter candidate among other things which makes it very appealing. If supersymmetry were a perfect symmetry then superparticles would be observed with the same masses as their standard model particle partners. This is not the case so supersymmetry must be a broken symmetry and the exact details and effects of this breaking are not fully understood. Because of this, the masses of the superpartners must be determined from experiment. The search for these particles is one of the primary goals of the LHC and of the ATLAS experiment.

The supersymmetric particles are given names based on their standard model partners. For each standard model fermion there is a corresponding sfermion which is named by adding an "s" (for scalar) before the particle's name. For example, the superpartner of the top quark (t) is the stop quark $(\tilde{t})$. Superpartners for bosons are named by appending "ino" to the particle's name such as gauginos for gauge bosons. In the Minimal Supersymmmetric Standard Model (MSSM), there are two complex Higgs doublets $H_u = (H_u^+, H_u^0)$ and $H_d = (H_d^0, H_d^-)$. The Higgs doublets have superpartners called higgsinos. Due to electroweak symmetry breaking, weak gauginos and higgsinos mix together to form mass eigenstates called charginos and neutralinos. Table 1 lists the standard model particles and their corresponding superpartners.[1] Superpartners are denoted symbolically by adding a tilde over the symbol of the corresponding standard model particle.

R-parity is a property defined as:

$$P_R = (-1)^{2s+3B+L} \tag{1}$$

with spin as s, baryon number as B and lepton number as L. R-parity conservation is introduced in SUSY in order to avoid lepton and baryon number violation interactions which haven't been observed to date in very high precision experiments. When R-parity is conserved, the lightest supersymmetric particle (LSP) will not be able to decay to standard model particles and will be stable. If the LSP is a charged particle then it will be possible to observe it in the detector. If the LSP is neutral, SUSY production will result in a large missing energy in the transverse plane of the detector which can be measured.

1.2 Weak Gaugino Production

Current searches for SUSY have not led to any discoveries and they have placed strong limits on the masses of 1^{st} and 2^{nd} generation squarks and gluinos. In many SUSY models consistent with large masses for these particles, the neutralinos and charginos will be light and accessible at LHC energies. Gauginos interact weakly so they can be produced in weak interactions at the LHC. Assuming that the $\tilde{\chi}_1^0$ is the LSP, any heavier weak gauginos that are produced will decay in a cascade to the $\tilde{\chi}_1^0$.

If sleptons are present, the heavier weak gauginos can decay via these which results in many leptons in the final state. Current analyses have already excluded a large region of the parameter space for these models. For this summer project I investigated the class of models where sleptons are heavy compared to the first neutralinos and charginos and where the $\tilde{\chi}_1^\pm$ and $\tilde{\chi}_2^0$ can only decay through weak interactions. This project was done with the group working on the analysis with a 3-lepton final state. With this final state and with this model, the SUSY process with the highest cross section is the production of $\tilde{\chi}_1^\pm\tilde{\chi}_2^0$ which then decays by a W and a Z boson to two $\tilde{\chi}_1^0$ particles (the LSP). A possible Feynman diagram for this process is shown in Figure 1.

In order to be able to effectively search for this decay mode, we assume that the $\tilde{\chi}_1^\pm$ and $\tilde{\chi}_2^0$ have identical masses. This means that there are only two free variables, the $\tilde{\chi}_1^\pm/\tilde{\chi}_2^0$ mass and the $\tilde{\chi}_1^0$ mass. Under this assumption the results can be translated to a 2D grid of these two variables and exclusion and discovery reaches can be drawn accordingly.

1.3 The LHC and the HL-LHC

The Large Hadron Collider (LHC) is currently the world's largest particle accelerator, operating at a center of mass energy of 8 TeV in 2012. By the end of 2012 the LHC is expected to collect 20 fb^{-1} of data. After this the machine will go into a long shutdown for a year where it will be upgraded to operate at the design energy of 14 TeV. The LHC will then run until it has collected a total of 300 fb^{-1} of data at this energy which will occur in approximately 2021.

The ATLAS detector is a multipurpose particle physics detector at the LHC with a cylindrical geometry. It is capable of measuring particles emitted in both

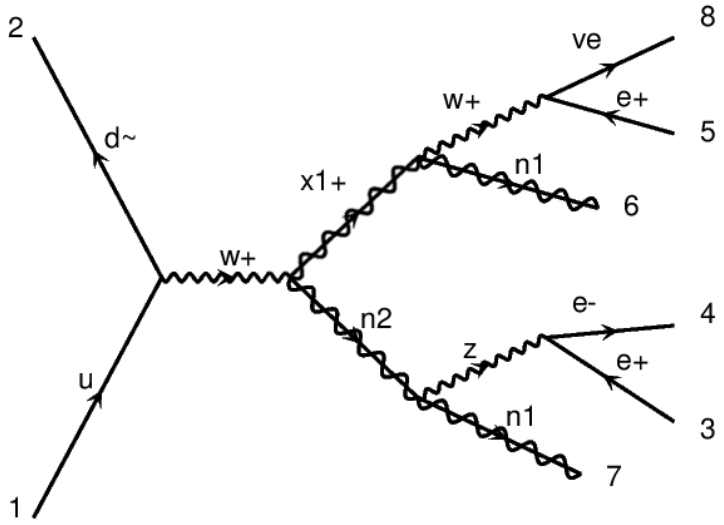

Figure 1: Feynman diagram for weak gaugino production with no sleptons and with a 3-lepton final state.

the forward and backward directions and uses a combination of tracking detectors and calorimeters to track and identify the particles that are produced in collisions. This project was done in the context of the ATLAS detector. The ATLAS tools and software were used to produce the results shown in this report and all of the results take the resolution and efficiency of the ATLAS detector into account.

The High Luminosity Large Hadron Collider (HL-LHC) is a proposed upgrade to the LHC which would occur after 2021.[2] This upgrade will increase the luminosity of the machine by around a factor of 5. The upgraded machine will operate at the same center of mass energy as the LHC of 14 TeV. The HL-LHC is expected to be run until it has collected 3000 fb^{-1} of data. This large dataset will be very useful for studying physics processes with low cross sections such as weak gaugino production. If SUSY is found at the LHC then it will be possible to study it to high precision with the HL-LHC. If SUSY is not found at the LHC then the HL-LHC will significantly extend the discovery and exclusion reaches for SUSY models.

There are many challenges with this new upgrade. Much research needs to be done to design and build new detectors and accelerator components that can operate at such high luminosities. On the physics analysis side, this luminosity means that the pile-up in the machine (number of interactions per bunch crossing) will be around 140. There will be very large numbers of particles in the detector which will require very good detector resolution and advanced reconstruction algorithms.

In order for this upgrade to be approved and funded, the physics results that it will be able to produce must be estimated. The production of weak gauginos without sleptons is a very good process to study in such a case since it is highly motivated and since it has a low cross section which is hard to study at the LHC. The additional statistics of the HL-LHC drastically improve the discovery and

exclusion reaches for this process. As part of my project I developed a set of selection criteria optimized for this signal and calculated the reaches at both the LHC and at the HL-LHC.

2 Monte Carlo generators

2.1 Introduction

The processes that are being studied at the LHC are very rare and only occur in a small number of interactions. The total cross-section at the LHC is on the order of 10^8 nb while processes such as $\tilde{\chi}_1^{\pm}\tilde{\chi}_2^0$ production are on the order of 10^{-5}-10^{-2} nb. Separating this signal from the background requires a very good understanding of the background processes. Monte Carlo generators are used to generate samples for all of the background processes that can produce signal-like events and signal regions selections are decided upon based on these. These samples can either be truth level only or can include a full detector simulation. Truth level samples contain only the four momentum of the generated particles whereas a full detector reconstruction includes effects such as pile-up and detector efficiency and resolution. For the weak gaugino to 3-lepton search, the most important background processes are WZ diboson production and $t\bar{t}$ production as will be discussed in Section 3.

In the ATLAS experiment, event generation and simulation is done using the Athena framework. This framework provides an interface to all of the different Monte Carlo generators and produces events in a common format. It can run GEANT4 simulations on generated events and can reconstruct and process the simulated events. Since different generators are best suited for different processes, this framework makes it relatively easy to perform an analysis using samples from many different generators.

For this project I learned how to use and ran several different Monte Carlo generators. The MadGraph[6] generator has an interface that requires only that initial and final states are specified and was used for getting estimates of cross sections before running other generators. MadGraph was also used to verify that all applicable diagrams were included when running other generators that have more strict process declarations. The Sherpa[7] generator also has an interface allowing for complex background processes with only the initial and final states specified and is good for simulating processes with large hard jet multiplicities. It was used to simulate diboson events with up to 3 jets. Alpgen was used in order to develop and investigate the properties of a potential filter for processes with fake leptons, such as Z bosons with jets, that would allow for simulation of higher luminosity samples. While this filter did not prove to be effective, it taught me how to use the Athena framework properly and how to create my own modules within the framework. More common background samples that are used by multiple groups were produced centrally using generators such as MC@NLO and were also used for this project.

While there are many generators to choose from for the background event simulation, there are only a few that can simulate supersymmetric processes such

as weak gaugino production. Both Herwig++[9] and Pythia[8] can simulate this process and were investigated. Herwig++ provides better agreement with data but is unable to run at 14 TeV with the current tunes. Hence the 14 TeV signal samples were generated using Pythia and the 7 and 8 TeV signal samples were generated using Herwig++.

2.2 k-factor calculations

Most of the Monte Carlo generators that were used only perform leading order (LO) calculations. More accurate results can be obtained by normalizing these cross sections to next-to-leading order (NLO) cross sections. NLO cross sections include either an additional loop or an additional outgoing hard jet compared to the LO cross section. The ratio of the NLO cross section over the LO cross section is called a k-factor.

NLO cross sections for the SUSY samples were calculated with Prospino2[11] which is a dedicated program for SUSY cross section calculations. MCFM[10] was used to calculate cross sections for the diboson background samples. Cross sections for other samples were available through the Standard Model group. The MSTW2008NLO PDF set was used for all MCFM calculations and the CT10 PDF set was also used for comparison and estimation of the PDF error. The CTEQ66 PDF set was used for the Prospino2 calculations.

The results of the Prospino2 calculations for $\tilde{\chi}_1^{\pm}\tilde{\chi}_2^0$ production for different values of the degenerate $\tilde{\chi}_1^{\pm}/\tilde{\chi}_2^0$ mass can be seen in Figure 2 for both 7 TeV and 14 TeV. The branching ratios of $\tilde{\chi}_1^{\pm}$ to $W\tilde{\chi}_1^0$ and $\tilde{\chi}_2^0$ to $Z\tilde{\chi}_1^0$ are assumed to be 100%. The cross sections of all of the generated SUSY samples are normalized to the Prospino2 cross sections.

For the diboson samples, the k-factors are not as straightforward to calculate. The samples to be used were generated using up to 3 jets but it is not possible to perform NLO calculations for this jet multiplicity. In order to provide the most accurate k-factor, the single Z boson samples were studied since MCFM can be used to calculate the inclusive NLO cross sections with up to 3 jets for these samples. Generator level cuts are applied to require Z boson masses of greater than 20 GeV. The results of these calculations are shown in Table 2.

As can be seen in this table, the k-factor is independent of jet-multiplicity within the errors of the PDF set for the Z boson sample. Hence the ratio of inclusive WZ+1jet NLO/LO will be used as a k-factor for the diboson 3-jets sample and should give a sample normalized to the WZ+3jet cross section within the errors of the PDF set. The final k-factors for all of the different diboson samples were calculated using this method and are shown in Table 3. The cross sections calculated for these k-factors were verified by comparing to results calculated by the ATLAS Standard Model group.

3 Background processes

Based on the 2011 3-lepton analysis, there are two main sources of background that must be taken into account in the 3-lepton channel. These are WZ diboson

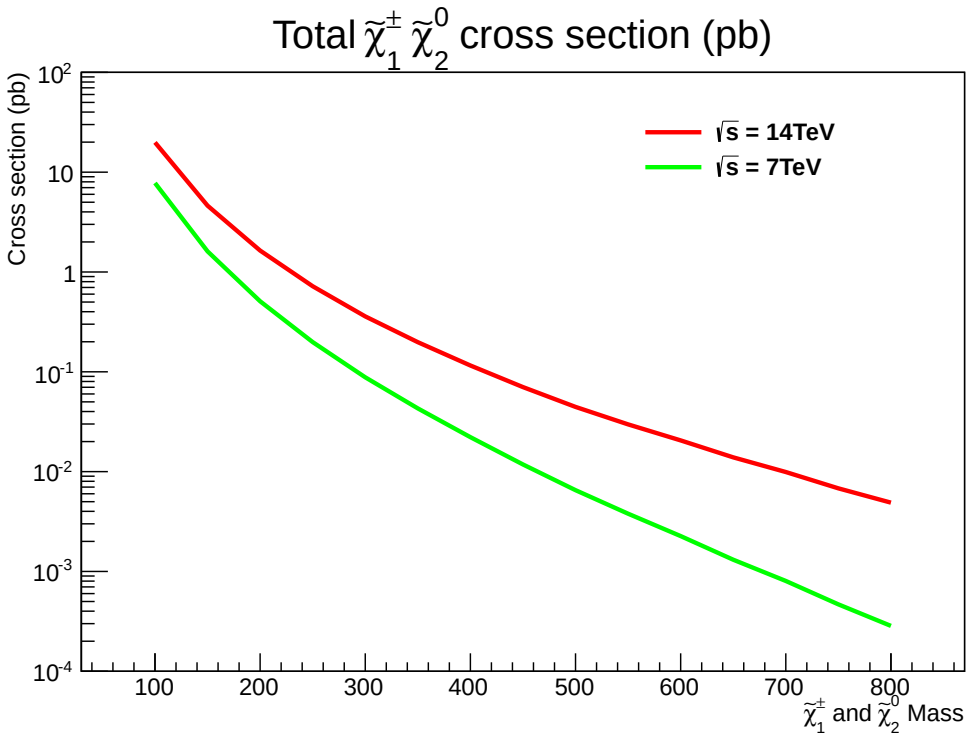

Figure 2: NLO cross sections for $\tilde{\chi}_1^{\pm}\tilde{\chi}_2^0$ production at the LHC calculated using Prospino2

production and $t\bar{t}$ production.

3.1 WZ diboson production

WZ diboson production is an irreducible background which produces 3 leptons and a neutrino. A possible Feynman diagram for this interaction can be seen in Figure 3. The cross-section for WZ boson production is approximately 50 pb at 14 TeV which is much larger than the 0.01-10 pb for $\tilde{\chi}_1^{\pm}\tilde{\chi}_2^0$ production seen in Figure 2 so hard cuts are needed, especially for the fb level signals.

The missing transverse energy ($\not{E}_T$) is calculated as the negative vector sum of the momenta of the visible particles. Since the initial protons in the collider had no energy in the transverse plane, any non-zero value of $\not{E}_T$ can be attributed to the presence of "invisible" particles, ones that don't interact with the detector. The only invisible particle in the WZ background is a single neutrino. For the SUSY signal interaction there is a neutrino along with two neutralinos in the final state. Hence cutting on the $\not{E}_T$ can provide good discrimination between the signal and background. The $\not{E}_T$ distribution for the background and signal points can be seen in Figure 4.

The transverse mass (M_T) of the W boson is another variable which provides good discrimination for this background. It is calculated by combining the $\not{E}_T$ and the properties of the lepton which not associated with the Z boson as follows:

$$M_T = \sqrt{2 \cdot \not{E}_T \cdot E_{T,l} \cdot (1 - \cos\phi)} \tag{2}$$

Table 2: Inclusive single Z boson cross sections (nb) and k-factors calculated using MCFM

	0-jet	1-jet	2-jet	3-jet
MSTW2008 NLO	21.4	27.8	30.0	30.7
MSTW2008 LO	22.4	29.3	32.1	33.1
CT10 NLO	21.4	27.8	29.8	30.7
CT10 LO	23.9	80.1	32.3	32.9
MSTW2008 NLO/LO	0.95	0.95	0.93	0.93
CT10 NLO/LO	0.90	0.92	0.93	0.93

Table 3: Diboson k-factors calculated using MCFM NLO 1-jet/Sherpa LO 1-jet

Sample	k-factor at 7 TeV	k-factor at 8 TeV
WW	1.085 ± 0.011	1.073 ± 0.012
WZ	1.083 ± 0.012	1.062 ± 0.012
ZZ	1.141 ± 0.013	1.106 ± 0.013

where ϕ is the angle between the $\not{E}_T$ and the transverse energy of the third lepton ($E_{T,l}$) in the transverse plane. The actual mass of the W boson can't be measured directly since the missing energy in the beam direction is not known. If the decay of the W boson is purely in the transverse plane, then the transverse mass will be equal to the true mass of the W boson. However, for decays which occur with a component along the beam direction, the relation $M_T <$ M will hold. Hence for the WZ signal the M_T distribution will have what is referred to as a Jacobian edge with a sharp decline in the number of events above the W boson mass. Due to the extra neutralinos in the SUSY signal events they will not experience this Jacobian edge and will typically have larger M_T values. The M_T distribution can be seen for a few points in Figure 4.

3.2 $t\bar{t}$ production

$t\bar{t}$ production is another important background since it has a very large cross section at approximately 1 nb at 14 TeV. A Feynman diagram for this interaction is shown in Figure 5. There are two b-quarks in this interaction, one of which must decay leptonically to end up with a 3-lepton final state. The other b-quark can produce a b-jet so b-vetoing will cut down this background significantly.

There is no Z boson in this interaction whereas there is one in the SUSY signal. Hence requiring that the reconstructed mass of two of the leptons is in the Z mass range cuts down the $t\bar{t}$ background significantly while having relatively little effect

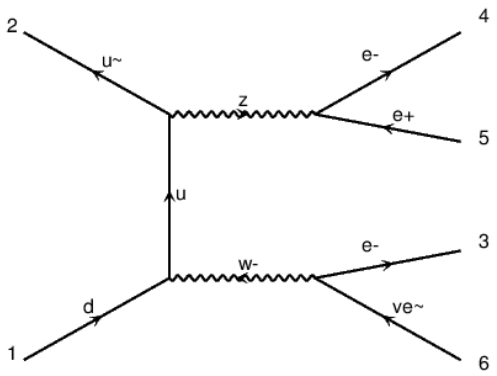

Figure 3: Feynman diagram for WZ diboson production

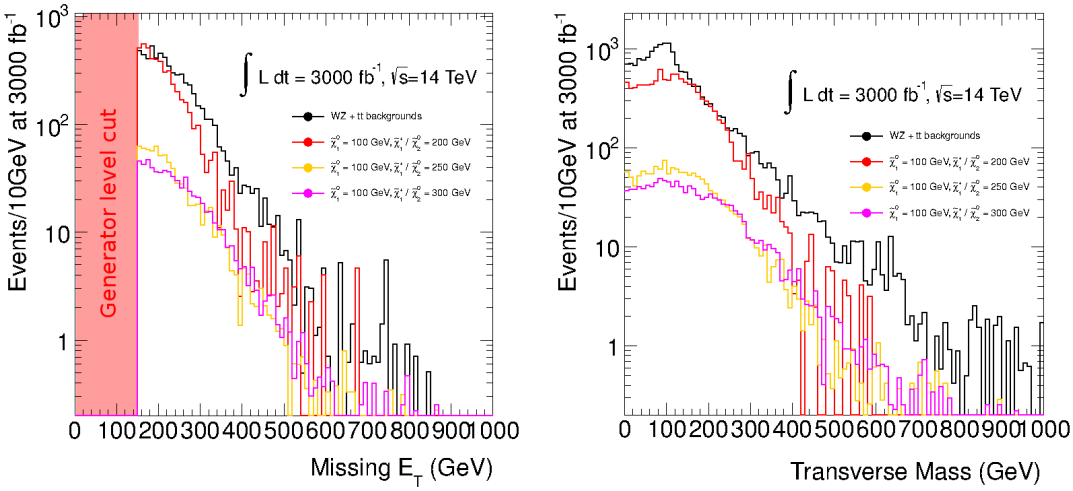

(a) $\not{E}_T$ (b) M_T

Figure 4: $\not{E}_T$ and M_T distributions

on the signal.

4 Optimization for the 2012, 8 TeV, 13 fb^{-1} data

4.1 Overview

A weak gaugino analysis is being performed on the 2012 data and will be run when approximately 13 fb^{-1} of data have been collected. For part of my project I worked on optimizing the signal selection for this analysis. This was done using a custom framework designed to run on truth level samples. A truth level analysis was done because only truth level samples were available for the 2012 analysis when this project was undertaken. The selection was done using rectangular cuts which were optimized using TMVA. The results were later confirmed using fully reconstructed samples validating the framework.

I wrote a set of custom codes to perform all of the tasks required for this analysis. The first set of scripts generates the truth samples using the Athena

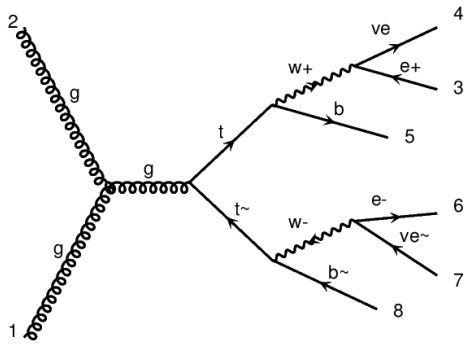

Figure 5: Feynman diagram for $t\bar{t}$ production

framework and calculates NLO cross sections using various programs. A custom code dubbed KyleCut then processes the truth level Monte Carlo data, calculates important kinematic variables, approximates detector resolution, applies a basic base cut flow and outputs a ROOT ntuple with event properties weighted for detector efficiencies. A set of codes then uses this ntuple to identify signal regions and to determine optimal sets of cuts for each region. Finally, a code combines the different signal regions and produces contour lines showing the exclusion and discovery reaches.

The method of truth level simulation is discussed in Section 4.2 and the method of calculating the significance is discussed in Section 4.3. The framework was verified against the 2011 results as shown in Section 4.4. The cut optimization using TMVA and final results are discussed in Section 4.5.

4.2 Truth Level Simulation

The signal optimization was performed only with the WZ background since the centrally produced $t\bar{t}$ sample was not ready when the analysis was being performed. The $t\bar{t}$ background had a much lower contribution to the final background than the WZ background in the 2011 analysis so the final results should not change significantly when it is added in.[3] Samples for the signal and the above backgrounds were produced centrally using Monte Carlo programs. Herwig++ was used for the signal and Sherpa was used for the WZ background. Cross sections were normalized to MCFM NLO calculations for the WZ sample and to Prospino2 NLO calculations for the signal samples.

A base selection was applied to each sample consisting of:

- 3 leptons
  - $p_T > 25/10/10$ GeV
  - $\eta < 2.6$
  - jet isolation
- b-jet veto

- Mass of a same flavour opposite sign pair (equal to reconstructed Z boson mass) > 20 GeV (due to a generator level cut on the WZ sample)

The studies were being performed at truth level so the samples themselves do not include the effects of detector resolution or pile-up. To account for this, the ATLAS European Strategy group has developed a set of smearing functions which can be applied to truth level simulations in order to estimate the new detector's response.[2] These were applied to all of the reconstructed particles assuming a pile-up of 25. Efficiencies were also applied to account for the success probability of factors such as the trigger and the b-jet veto and a weight was given to each event which takes these efficiencies into account.

4.3 Significance Calculation

Significance is a statistical value used to determine at what level a set of observations are consistent with new signal rather than just a background. A basic measure of significance would be the ratio of signal to the square root of background or $S/\sqrt{B}$. However, this is a rather simplistic definition which does not take into effects like systematic uncertainties.

The exclusion and discovery reaches were calculated using the Z_n significance algorithm. The Z_n calculation takes systematic uncertainties into account; these were estimated to be 30%. The exclusion reach is defined as the region for which a signal is excluded at a 95% confidence level. This corresponds to a Z_n value of greater than 1.645. The discovery reach is defined as the region for which a "5-sigma" discovery can be made. Hence it corresponds to the region with a Z_n value of greater than 5.

4.4 Verification of 2011 Results

To verify that this method of truth level analysis is correct the 2011 cuts were reproduced. The old 2011 results and the reproduced results with the new framework are shown in Figure 6. The 2012 grid is at 8 TeV whereas the 2011 grid is at 7 TeV so some differences are to be expected between the two grids. Nevertheless the results are consistent and the new truth level framework gives approximately the same exclusion reach as the full framework used previously.

4.5 Cut optimization using TMVA

Rectangular cuts were for this analysis. These were optimized using the TMVA "Cuts" option. The following variables were entered into TMVA:

- $\not{E}_T$
- M_T
- p_T of the leading lepton
- Mass of reconstructed Z boson

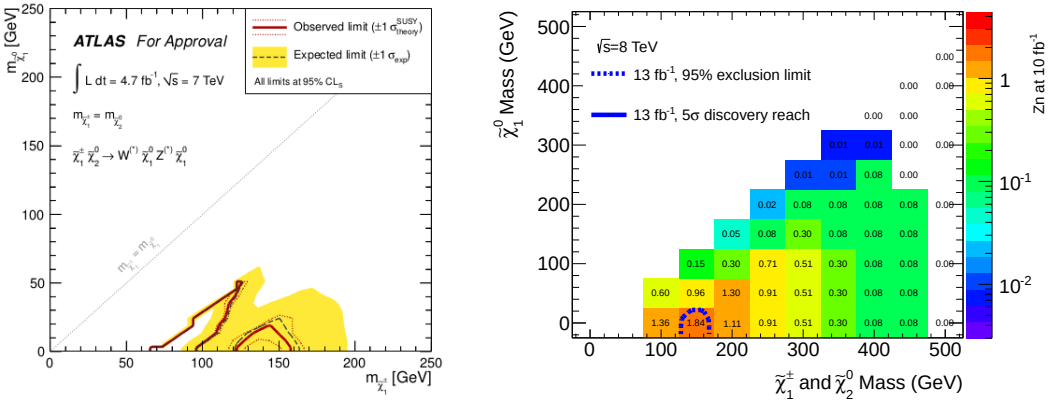

(a) 2011 results (7 TeV, 5 fb^{-1})

(b) Significance in new framework with 2011 cuts (at 8 TeV, 5 fb^{-1})

Figure 6: Verification of the truth level analysis framework using the 2011 cuts.

- p_T of the reconstructed Z boson
- $\Sigma\ E_T$

TMVA runs through these variables and automatically finds the ones that give the best sensitivity. It varies cuts on all of the listed variables in order to determine which ones are the most effective to cut on and which combinations of cuts work best. To do this, it scans through a list of signal efficiencies and finds the set of cuts that lead to the lowest background efficiency for each given signal efficiency. After this is done, the best signal efficiency can be determined by picking the one that gives the highest significance and by using the cuts that are associated with it.

Two data points were chosen to select a set of cuts for. These were $\tilde{\chi}_1^0 = 100$ GeV, $\tilde{\chi}_2^0 = 200$ GeV for the low mass splitting and $\tilde{\chi}_1^0 = 50$ GeV, $\tilde{\chi}_2^0 = 200$ GeV for the high mass splitting. The distribution of these kinematic variables for the two data points can be seen in Figure 7. These figures show probability distributions and the signal is only approximately 2% of the background for these points. These diagrams show that discrimination for the low mass splitting is very difficult and there are no easy cuts that help significantly. The high mass splitting has long tails for the signal in both the $\not{E}_T$ and M_T distributions which can be cut on.

Figure 8 shows the significance as a function of signal efficiency for both training data points. For the low mass splitting, the cuts do not help at all and the optimal significance occurs when no cuts on the given variables are applied. For the high mass splitting, the significance peaks around a signal efficiency of 0.2. This corresponds to the cuts of:

- $\not{E}_T > 95$ GeV
- $M_T > 115$ GeV

Additionally, in order to reduce the effect of the $t\bar{t}$ background further, a pair of same flavour opposite sign leptons with a reconstructed mass within 10 GeV of the Z mass are required. This ensures that the top background is negligible which

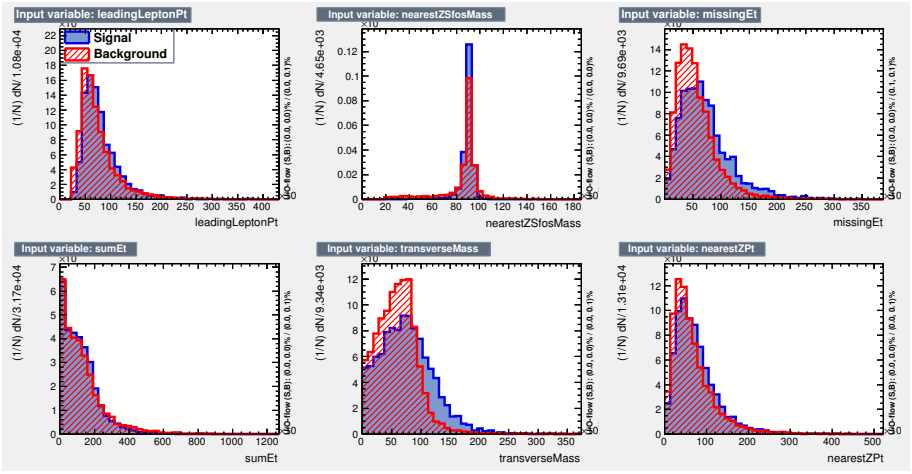

(a) 100/200 (low mass splitting)

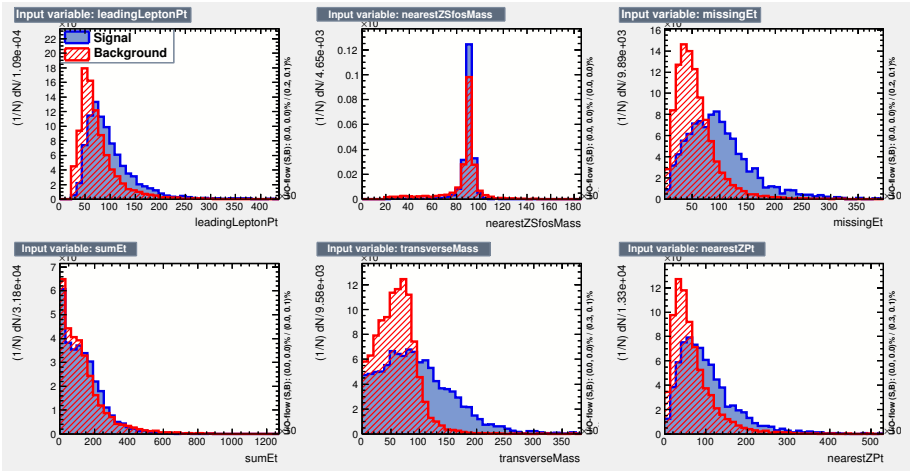

(b) 50/200 (high mass splitting)

Figure 7: Kinematic variable distributions for the two training points

is important since these kinematic cuts reduce the WZ background to just 1.5 signal events.

As a result, two signal regions are recommended to be used after this analysis. The first with no cuts other than the base cuts to target low mass splitting regions and the second with the kinematic cuts described above to target the high mass splitting regions.

The results of these cuts are shown in Figure 9. The exclusion reach using these cuts is extended along a diagonal to a $\tilde{\chi}_1^0$ mass of 50 GeV and a $\tilde{\chi}_2^0$ mass of 200 GeV. This is significantly more than what was achieved in the 2011 analysis and should be studied further with the fully simulated samples. These cuts provide a good starting point for these additional studies. As the 2011 results were reproduced well using this truth framework these cuts should work well on the 2012 data too.

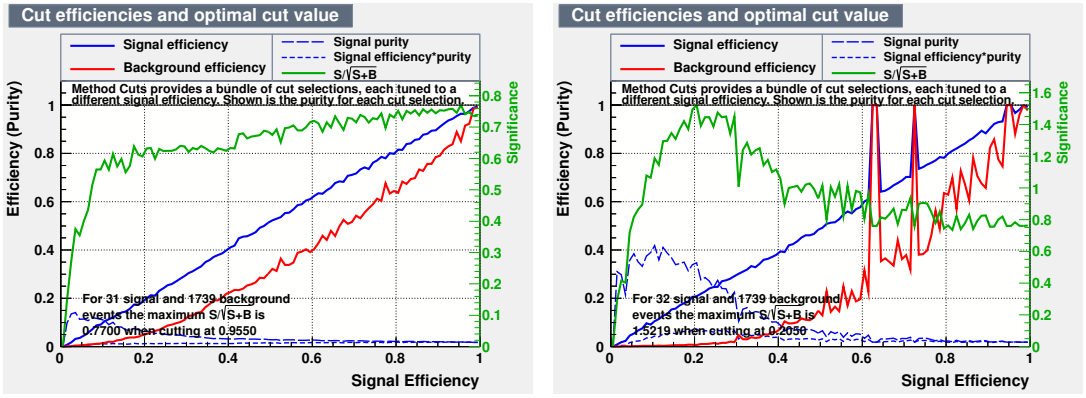

(a) 100/200 (low mass splitting) (b) 50/200 (high mass splitting)

Figure 8: Significance as a function of signal efficiency for the two training points

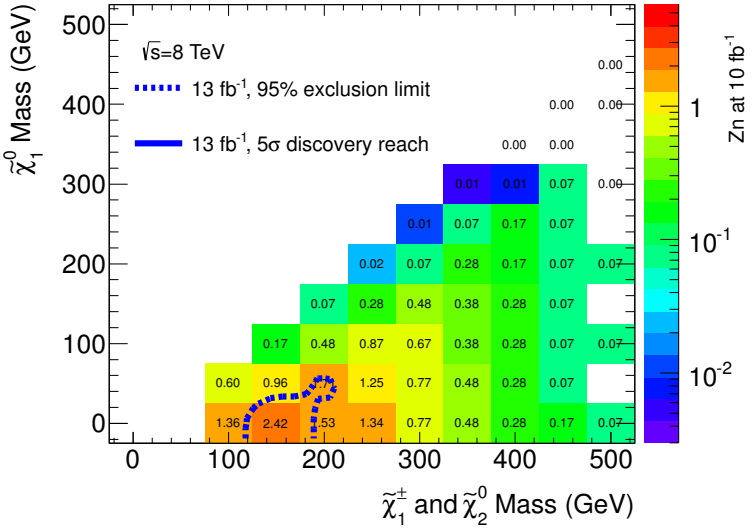

Figure 9: Expected discovery and exclusion reaches for the 2012 analysis with 13 fb^{-1} of data at 8 TeV

5 Optimization for the HL-LHC

5.1 Overview

In order to determine the reach of the HL-LHC for this model, a suitable signal selection must be found which takes advantage of the high luminosity of the HL-LHC. The large amount of data means that very tight cuts can be performed on the background as long as a few signal events still pass the signal selection. The analysis was performed using the same framework used for the 2012 optimization in Section 4.

The changes from the 2012 truth level simulation are discussed in Section 5.2. A Boosted Decision Tree was implemented to optimize the signal selection and is discussed in Section 5.3. The final reach of both the LHC and HL-LHC for this model can be found in Section 5.4.

5.2 Truth Level Simulation

The signal and WZ background samples were produced following the same procedure that was used for the 2012 analysis samples although Pythia was used for the signal grid instead of Herwig++ as discussed in section. The signal grid and WZ background samples were generated locally using the UBC ATLAS Tier 3 resources since they were not required for any other analyses. A centrally produced $t\bar{t}$ sample was used which was generated using MC@NLO. Cross sections for the $t\bar{t}$ sample were normalized to NLO cross-sections from the ATLAS Standard Model group.

Base cuts were applied similar to those in the 2012 analysis. However, since the WZ sample generated locally was much smaller than the centrally produced one for the 2012 dataset, a $\not{E}_T$ cut of 150 GeV was introduced at the generator level on that sample. This cut was applied to all of the other samples as well. All of the other base cuts described in 4.2 were also applied. The ATLAS European Strategy smearing functions were used as in the 2012 analysis but assuming a pile-up of 140. Additionally, the systematic error estimate for the Zn calculation was lowered to 20% based on estimates from the European Strategy group.

5.3 Applying a Boosted Decision Tree

The variables that were previously discussed such as those shown in Figure 4 each help with discriminating the signal from the background but the signal is still usually much smaller than the background after a single variable cut for the SUSY masses observable at the HL-LHC. In order to increase sensitivity, cuts can be applied on multiple variables by using a Boosted Decision Tree. This consists of generating many weighted trees, each with a few different cuts optimized to pick out signal from background. An example of such a tree is shown in Figure 10. The outputs of all of these trees are combined to give a score between -1 to 1 to each event called the BDT score. A value of -1 indicates that the event is most likely background whereas a value of 1 indicates that the event is most likely signal. Figure 11 shows the BDT score distribution for the background and the 200/700 signal point. A cut is then applied to the BDT score in order to optimize the significance and all events that fall below the BDT score cut are rejected.

The following variables were used to train the BDT:

- $\not{E}_T$
- M_T
- p_T of the leading lepton
- p_T of the softest lepton
- Mass of reconstructed Z boson
- p_T of the reconstructed Z boson
- Σ E_T

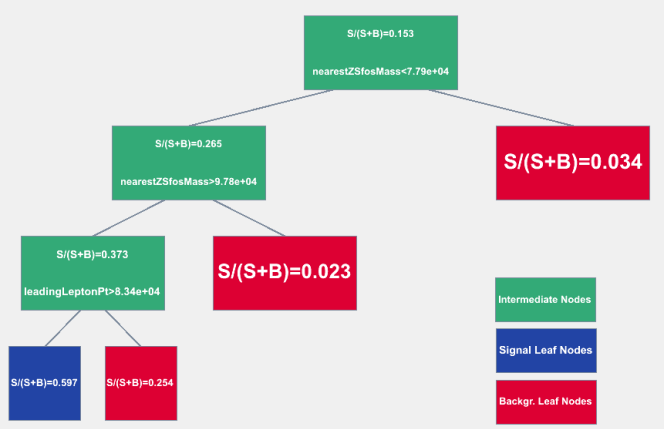

Figure 10: Example of a tree from a BDT produced using TMVA

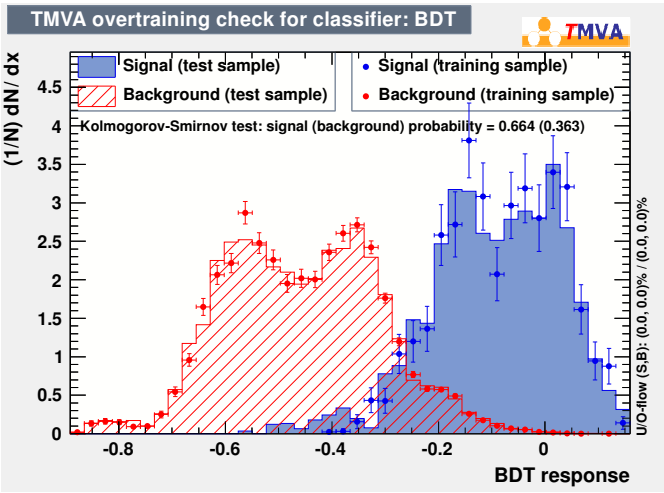

Figure 11: BDT score distribution for a BDT trained on the 200/700 data sample

The ROOT TMVA package was used to train two different BDTs.[5] One BDT was trained for samples with small differences between the $\tilde{\chi}_1^0$ and the $\tilde{\chi}_2^0$ masses using the $\tilde{\chi}_1^0 = 200$ GeV, $\tilde{\chi}_2^0 = 300$ GeV data point. A second BDT was trained for large mass splittings using the 200/700 data point. Using two BDTs significantly improves the sensitivity since the $\not{E}_T$ and M_T distributions are similar to the WZ distribution for the low mass splittings but very spread out for the high mass splittings. By using two BDTs, the analysis is optimized for both of these regions. The results of these two BDTs are combined by taking the output of whichever BDT has the highest significance at each point. Figure 12 shows which BDT was chosen for each signal point using this method.

5.4 Reach of the HL-LHC and LHC

This same procedure was followed for both 300 fb^{-1} and 3000 fb^{-1} datasets to estimate the reach of the HL-LHC and of the LHC. The results of this process are shown in Figure 13. This grid shows the final discovery reach and exclusion reach for both the LHC and the HL-LHC.

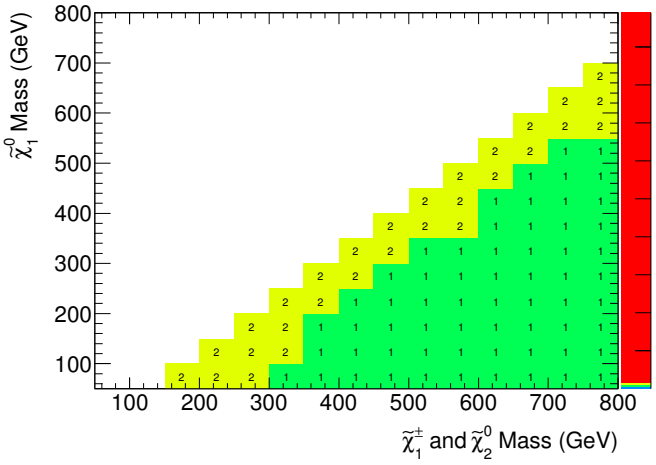

Figure 12: Illustration of which BDT was chosen for each signal point. The 200/700 trained BDT is labelled 1 and is shown in green. The 200/300 BDT is labelled 2 and is shown in yellow

The discovery reach increases quite significantly from 300 fb^{-1} to 3000 fb^{-1}. The entire region with the $\tilde{\chi}_1^0$ mass less than approximately 300 GeV can be discovered at the 5-sigma level with 3000 fb^{-1} of data and the exclusion reach extends to $\tilde{\chi}_1^0$ masses of over 450 GeV. Figure 14 shows the distribution of the $\not{E}_T$ for two signal points and for the background for events that passed the BDT and could be used for further studies if an excess is observed.

This project was done as part of the ATLAS European Strategy HL-LHC upgrade studies. The results of this analysis were included in the associated ATLAS Note ATL-PHYS-PUB-2012-001.[2]

6 Conclusion

A SUSY model was investigated where the only light SUSY particles are weak gauginos and with a final state with 3 leptons and missing transverse energy. Samples were generated using Monte Carlo techniques and were studied at truth level using smearing functions and efficiencies to account for detector resolution. These samples were used to optimize selections and determine the expected exclusion and discovery reaches for the 2012, 13 fb^{-1}, 8 TeV LHC run, the full 300 fb^{-1}, 14 TeV LHC run and the 3000 fb^{-1}, 14 TeV HL-LHC run.

For the 2012 LHC run, a set of cuts was optimized using TMVA. These resulted in two signal regions, one with just the base cuts and one with cuts of 95 GeV on the $\not{E}_T$ and 115 GeV on the M_T. Combining the results of these two signal regions gives an exclusion reach up to masses of 50 GeV for the $\tilde{\chi}_1^0$ and 200 GeV for the $\tilde{\chi}_2^0$.

For the full LHC and HL-LHC runs, a set of BDTs was trained using TMVA to optimize sensitivity for both the low mass splitting region and the high mass splitting region. The output of these BDTs was combined and the Zn algorithm was used to calculate the significance and determine reaches. The HL-LHC was

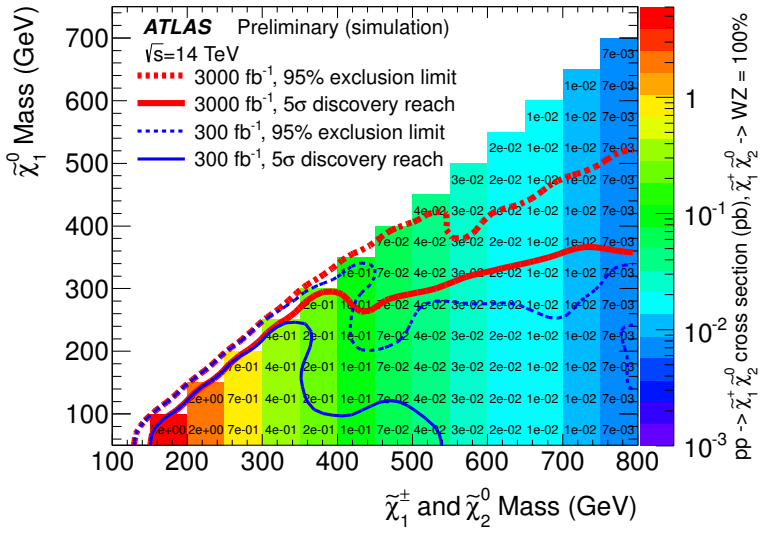

Figure 13: Discovery and exclusion reaches for the LHC and for the HL-LHC

found to have a much larger discovery reach than the LHC. A model with a $\tilde{\chi}_1^0$ mass of less than approximately 300 GeV can be discovered at the 5-sigma level with 3000 fb^{-1} of data and a model with a $\tilde{\chi}_1^0$ mass of less than 450 GeV can be excluded at the 95% confidence level.

7 Acknowledgements

I am sincerely thankful to Dr. Colin Gay for giving me the opportunity to join his lab and work on this project. I would also like to thank Dr. William Trischuk for organizing the IPP CERN Summer Student programme which sponsored my trip to CERN. I thank NSERC for their USRA program and the University of British Columbia which provided financial support for my work this summer. I am very grateful to Zoltan Gecse and to Anadi Canepa for their guidance and support and to Sam King for his help and for his constant enthusiasm and cheeriness.

References

[1] Martin, Stephen P., "A Supersymmetry Primer", arXiv:hep-ph/9709356v6, 2011

[2] ATLAS Collaboration, The, "Physics at a High-Luminosity LHC with ATLAS", ATL-PHYS-PUB-2012-001, 2012

[3] ATLAS Collaboration, The "Search for supersymmetry in events with three leptons and missing transverse momentum in sqrt(s) = 7 TeV pp collisions with the ATLAS detector", arXiv:1204.5638, 2012

[4] Baer, H. et al., "WZ plus missing-ET signal from gaugino pair production at LHC7", arXiv:1201.5382, 2012

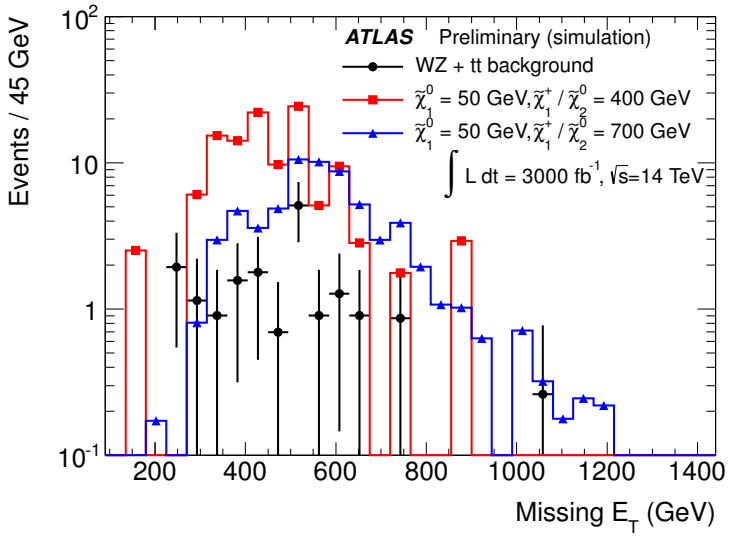

Figure 14: $\not\!\!E_T$ distribution for events passing the BDT

[5] Hoecker, A. et al., "TMVA: Toolkit for Multivariate Data Analysis", arXiv:physics/0703039, 2007

[6] Alwall, J. et al., "MadGraph 5 : Going Beyond", arXiv:1106.0522v1, 2011

[7] Gleisberg, T. et al., "Event generation with SHERPA 1.1", arXiv:0811.4622v1, 2008

[8] Sjostrand, T. et al., "PYTHIA 6.4 Physics and Manual", arXiv:hep-ph/0603175v2, 2006

[9] Bahr, M. et al., "Herwig++ Physics and Manual", arXiv:0803.0883v3, 2008

[10] Campbell, J., Ellis, R. K. and Williams, C., "A Monte Carlo for FeMtobarn processes at Hadron Colliders", 2012

[11] Beenakker, W. et al, "The Production of charginos / neutralinos and sleptons at hadron colliders." Phys. Rev. Lett. 83, 3780-3783, 1999